

# ON THE USE OF MIR REFLECTANCE FOR BURNED AREA IDENTIFICATION

Renata Libonati<sup>(1),(3)</sup>, Carlos C. DaCamara<sup>(1)</sup>, José Miguel C. Pereira<sup>(2)</sup>, Alberto W. Setzer<sup>(3)</sup> and Leonardo F. Peres<sup>(3)</sup>

<sup>(1)</sup> University of Lisbon, CGUL, IDL, Campo Grande, Ed. C8 – 3º Piso, 1749-016 Lisbon, Portugal

<sup>(2)</sup> Department of Forestry, Instituto Superior de Agronomia, Tapada da Ajuda, 1349-017 Lisbon, Portugal

<sup>(3)</sup> Instituto Nacional de Pesquisas Espaciais, Centro de Previsão do Tempo e Estudos Climáticos, Rod. Presidente Dutra, km 40, 12630-000, Cachoeira Paulista, Brazil

[rlsantos@fc.ul.pt](mailto:rlsantos@fc.ul.pt); [cdcamara@fc.ul.pt](mailto:cdcamara@fc.ul.pt); [jmcpereira@gmail.com](mailto:jmcpereira@gmail.com); [asetzer@cptec.inpe.br](mailto:asetzer@cptec.inpe.br); [lperes@cptec.inpe.br](mailto:lperes@cptec.inpe.br)

## Abstract

Middle infrared (MIR) surface reflectance is sensitive to changes in vegetation cover but is not affected by the presence of most aerosols. This characteristic makes of MIR an especially adequate spectral band for burned area identification over regions affected by the presence of heavy smoke layers due to the biomass burning. However use of the MIR region brings up the difficult problem of distinguishing, in a single measurement, between a diversity of radiance sources, namely the thermal emission and the solar reflection from the atmosphere and the surface. The aim of the present study is to assess the potential of MIR to identify burned scars over tropical environments. Special attention will be devoted to the method proposed by Kaufman and Remer (1994) whose performance will be compared against results obtained by inverting the general radiative transfer equation.

## INTRODUCTION

An accurate identification of burnt areas is of paramount importance in a wide range of studies ranging from the greenhouse effect, the destruction of stratospheric ozone and land emissivity up to ecosystem stability and biodiversity. Current methods for detecting burned areas have mainly relied on information in the red and near infrared (NIR) regions of the electromagnetic spectrum. However, both red and NIR channels are especially sensitive to aerosol scattering and absorption in the atmosphere. Usage of these two channels for burned area detection may therefore bring unsatisfactory results over tropical regions such as Amazonia, because of the presence of heavy smoke layers due to the biomass burning. A possible way to mitigate the aerosol effects associated to biomass burning is by using the middle infrared (MIR) part of the spectrum, since it is also affected by vegetation changes but is not sensitive to the presence of most aerosols. However use of MIR brings up the hard problem of distinguishing, in a single measurement, between a diversity of radiance sources, namely the thermal emission and the solar reflection from the atmosphere and the surface. Methods that take into account the major components of the MIR signal have to rely on information from auxiliary datasets (e.g. atmospheric profiles) and require large computational means (e.g. for radiative transfer computations). A simple method was proposed by Kaufman and Remer in 1994 where different assumptions are made that allow separating the thermal and solar components of the MIR signal. This method does not require heavy numerical computations and presents the major advantage of avoiding the use of auxiliary datasets. It was first designed to identify dense, dark vegetation areas in mid-latitude environments and has been widely used in burned area discrimination. However, to the best of our knowledge, no assessment has been made on the required accuracy of the MIR reflectance retrievals to adequately identify burnt areas in tropical environments. Accordingly, in this work we present a sensitivity study aiming to assess the performance of existing methods, using simulations of

observed radiances from a radiative transfer model. Obtained results suggest that Kaufman and Remer's method does not provide accurate enough estimates of MIR reflectance to allow discriminating burned areas in tropical environments. The present study represents the first step towards building up an improved algorithm that will overcome the identified difficulties in the process of burned area discrimination using MIR reflectances.

## PHYSICS OF THE PROBLEM

The top of the atmosphere (TOA) radiance in the MIR channel as measured by a satellite in clear-sky conditions may be written in the form of the following energy balance equation:

$$L_{\text{MIR}} = t_{\text{MIR}} \rho_{\text{MIR}} \frac{E_{0\text{MIR}}}{\pi} \mu_0 + \tau_{\text{MIR}} \varepsilon_{\text{MIR}} B(\lambda_{\text{MIR}}, T_s) + \tau_{\text{MIR}} \rho_{\text{MIR}} \bar{L}_{\text{atm, MIR}} \downarrow + L_{\text{atm, MIR}} \uparrow + L_s. \quad (1)$$

In the above expression,  $t_{\text{MIR}}$  is the two-way total atmospheric transmittance (sun-surface-sensor);  $\rho_{\text{MIR}}$  is the surface reflectance;  $E_{0\text{MIR}}$  is the exo-atmospheric irradiance;  $\mu_0$  is the cosine of the solar zenith angle (SZA);  $\tau_{\text{MIR}}$  is the one-way total atmospheric transmittance (surface-sensor);  $\varepsilon_{\text{MIR}}$  is the surface emissivity;  $B(\lambda_{\text{MIR}}, T_s)$  is the emitted radiance given by Planck's function for the surface temperature  $T_s$  and the central wavelength  $\lambda_{\text{MIR}}$ ;  $\bar{L}_{\text{atm, MIR}} \downarrow$  is the hemispherically averaged atmospheric downward thermal emission;  $L_{\text{atm, MIR}} \uparrow$  is the atmospheric upward thermal emission and  $L_s$  is the term associated with atmospheric scattering.

The first term on the right-hand side of (1) represents the solar radiance that is attenuated by the atmosphere in its downward path, reflected by the surface and again attenuated in its upward path to the sensor. The second term represents the radiance emitted by the surface that is attenuated by the atmosphere. The third term denotes the downward atmospheric radiance that is reflected by the surface and then attenuated in its upward path to the sensor. The fourth term represents the radiance emitted by the atmosphere towards the sensor. Finally, as previously mentioned, the last term is associated with atmospheric scattering.

Assuming the Earth's surface behaves as a Lambertian emitter-reflector, surface reflectance and emissivity are related as:

$$\rho_{\text{MIR}} = 1 - \varepsilon_{\text{MIR}} \quad (2)$$

Using equation (2) and neglecting the atmospheric scattering term  $L_s$ , the solution of equation (1) is given by:

$$\rho_{\text{MIR}} = \frac{L_{\text{MIR}} - \tau_{\text{MIR}} B(\lambda_{\text{MIR}}, T_s) - L_{\text{atm, MIR}} \uparrow}{t_{\text{MIR}} \frac{E_{0\text{MIR}}}{\pi} \mu_0 - \tau_{\text{MIR}} B(\lambda_{\text{MIR}}, T_s) + \tau_{\text{MIR}} L_{\text{atm, MIR}} \downarrow} \quad (3)$$

Problems encountered in estimating MIR reflectance based on the radiative transfer equation (RTE), i.e. equation (3), originate from i) the diversity of radiance sources (e.g., thermal emission and solar reflection from atmosphere and surface) in a single measurement, ii) the uncertainties in the land surface temperature, iii) the atmospheric correction and iv) the angular effects. Using equation (3) to estimate surface MIR reflectance is therefore a complex task that requires "real-time" auxiliary datasets (e.g. atmospheric profiles) and major computational facilities (e.g. for radiative transfer computations). Kaufman and Remer (1994) proposed a simple methodology that is based on the studies of Gesell (1989) and Ruff & Gruber (1983), who pointed out the existence of a mutual

compensation of attenuation and thermal emission terms, so that both atmospheric transmittances (i.e.  $t_{\text{MIR}}$  and  $\tau_{\text{MIR}}$ ) may be assumed to be equal to unity and both the atmospheric downward and upward thermal emission terms may be neglected. A closer look at equation (3) will help understanding the meaning of these assumptions. Let us first consider the numerator of the second hand term of equation (3), and let us suppose that we neglect the atmospheric upward emission term ( $L_{\text{atm,MIR}} \uparrow$ ). Since  $L_{\text{MIR}}$  is fixed, the only way to compensate the neglected term is by increasing the contribution of the remaining term  $\tau_{\text{MIR}} B(\lambda_{\text{MIR}}, T_S)$ . This is only possible by increasing the atmospheric transmittance  $\tau_{\text{MIR}}$ , in particular by setting it equal to unity. Now, taking into consideration the denominator, let us suppose that we neglect the atmospheric downward emission term ( $\bar{L}_{\text{atm,MIR}} \downarrow$ ). Then, in order to compensate the neglected term, we have either to decrease the contribution of term  $\tau_{\text{MIR}} B(\lambda_{\text{MIR}}, T_S)$  or to increase the contribution of term  $t_{\text{MIR}} \frac{E_{\text{OMIR}}}{\pi} \mu_0$ . However the first possibility is ruled out by the fact that we have already assumed that  $\tau_{\text{MIR}} = 1$ . Therefore we have to increase the contribution of the term  $t_{\text{MIR}} \frac{E_{\text{OMIR}}}{\pi} \mu_0$  by increasing  $t_{\text{MIR}}$ , in particular by setting it equal to unity. It may be noted that setting both  $t_{\text{MIR}}$  and  $\tau_{\text{MIR}}$  to unity does indeed lead to the required increase that compensates neglecting the term  $\bar{L}_{\text{atm,MIR}} \downarrow$ . This is due to the fact that, in general,  $t < \tau$  and therefore the assumption  $t_{\text{MIR}} = \tau_{\text{MIR}} = 1$  leads to a greater increase in the contribution of term  $t_{\text{MIR}} \frac{E_{\text{OMIR}}}{\pi} \mu_0$  than in term  $\tau_{\text{MIR}} B(\lambda_{\text{MIR}}, T_S)$ .

Considering the above mentioned assumptions, equation (3) becomes:

$$\rho_{\text{MIR}} = \frac{L_{\text{MIR}} - B(\lambda_{\text{MIR}}, T_S)}{\frac{E_{\text{OMIR}}}{\pi} \mu_0 - B(\lambda_{\text{MIR}}, T_S)} \quad (4)$$

Kaufman & Remer (1994) introduced another approximation for equation (4), using the brightness temperature from a thermal infrared (TIR) band ( $T_{\text{B,TIR}}$ ) as a surrogate for  $T_S$ , leading to:

$$\rho_{\text{MIR}} = \frac{L_{\text{MIR}} - B(\lambda_{\text{MIR}}, T_{\text{B,TIR}})}{\frac{E_{\text{OMIR}}}{\pi} \mu_0 - B(\lambda_{\text{MIR}}, T_{\text{B,TIR}})} \quad (5)$$

Since the brightness temperature is usually lower than the surface temperature, using a temperature lower than  $T_S$  (such as  $T_{\text{B,TIR}}$ ) tends to compensate the net effect resulting from the assumptions that the contributions from atmospheric emission are null and that the transmission functions are both equal to unity. Kaufman & Remer (1994) estimated the accuracy of equation (5) to be around 0.01 to 0.02 for a mid-latitude atmosphere in the range of emissivities typical of a variety of vegetation and soils (0.94 – 1.00). Equations (4) and (5) have also been used in a number of environment studies (e.g. Barbosa et al., 1999; Boyd, 1999; Boyd & Duane, 2001; Holben & Shimabukuro, 1993; Pereira, 1999; Roy et al., 1999; Cihlar et al., 2004). However to our knowledge, no assessment has been made on the cost of using the above mentioned simplifications when studying burned areas in tropical environments.

The usefulness of the approach proposed by Kaufman and Remer (1994) was evaluated by comparing results obtained using the “simplified” equation (5) against those based on the “full” equation (3), which requires using a radiative transfer model. The two procedures, i.e. the one based on Kaufman and Remer’s equation (5) and the one based on the inversion of the radiative transfer equation (3) will be hereafter referred to as KFE and RTE, respectively.

## RESULTS AND DISCUSSION

We have performed radiative transfer simulations for a wide variety of atmospheric, surface and geometry conditions as observed by the MODIS sensor. Simulations of observed radiances of MODIS channels 20 (3.66 - 3.84  $\mu\text{m}$ ) and 31 (10.78 - 11.28  $\mu\text{m}$ ), were obtained using MODTRAN-4 radiative transfer model (Berk et al., 2000). The atmospheric contribution was computed for three geographical-seasonal model atmospheres stored in MODTRAN-4, namely Mid-Latitude Summer (MLS), Mid-Latitude Winter (MLW), and Tropical (TRO), that allow covering a wide range of atmospheric conditions, with water vapor content of 0.85, 2.92 and 4.11  $\text{g cm}^{-2}$  and 2m-air temperature ( $T_a$ ) of 272.2, 294.2 and 299.7 K, respectively. The values prescribed for the land surface temperature were based on the 2m air temperature of each profile which was increased from  $T_a+0$  to  $T_a + 30.0$  K in steps of 1.0 K, totalizing 31 different values. The sun-view geometry was characterized by 3 view zenith angles (VZA), i.e.,  $0^\circ$ ,  $30^\circ$  and  $60^\circ$ , and 4 SZA, i.e.,  $0^\circ$ ,  $30^\circ$ ,  $45^\circ$  and  $60^\circ$ . We have selected 2 types of different surfaces representing vegetated and burned areas. Surface emissivity values were based on information from charcoal and vegetation emissivity spectra. Charcoal data were provided by the NASA Jet Propulsion Laboratory with a Beckman UV5240 spectrophotometer, based on samples of fire residues collected at Alta Floresta, state of Mato Grosso, Brazil. The dataset of vegetation emissivity was obtained from MODIS-UCSB spectral library. The vegetation dataset includes most vegetation types (Salisbury & D'Aria, 1994; Peres & DaCamara, 2005), with surfaces emissivities varying from 0.96 to 0.99 in MIR channel. The charcoal dataset is composed by fire residues of 4 different kind of tropical trees. In order to reduce the number of computations, we opted to restrict to the two mean spectral curves of the vegetation and the charcoal datasets.

Besides the errors inherent to the inversion procedure and the adopted approximations, the accuracy of KFE will depend on the instrument performance that is quantified by the radiometric noise. Conversely, the accuracy of RTE will depend on, i) the anisotropic behavior of the surface, ii) the atmospheric scattering effects, iii) the error due to the inversion procedure. iv) the uncertainties on the atmospheric profile, which are usually due to the errors in temperature and humidity profiles, v) the error due to instrument performance, which is quantified by the radiometric noise and vi) the error due to uncertainties in the retrieval of  $\rho_{\text{MIR}}$ . The first two sources of error will not be taken into account in our study, i.e., results were generated considering that the surface is Lambertian, that there is no significant atmospheric scattering. The assumption of a Lambertian surface is justified since angular dependences of the surface reflectance spectra used in this work are not available.

As we have pointed out early, RTE neglects the effects of atmospheric scattering. Figure 1 shows the box plot of the contributions to the MIR signal due to atmospheric scattering, surface reflection, surface emission and atmospheric emission for TRO atmospheric profile, considering all simulations. The lower and upper lines of the "box" are the 25th and 75th percentiles of the sample. The distance between the top and bottom of the box is the interquartile range. The line in the middle of the box is the sample median. Assuming no outliers, the maximum of the sample is the top of the upper whisker. The minimum of the sample is the bottom of the lower whisker. It may be noted from Figure 1, that the contribution of atmospheric scattering to the total signal ranges from 0.001 to 0.01% and is orders of magnitude smaller than the other terms. A contribution this small is negligible and will not introduce significant errors in the retrieval of surface reflectance. Similar results were found for MLS and MLW atmospheric profiles.

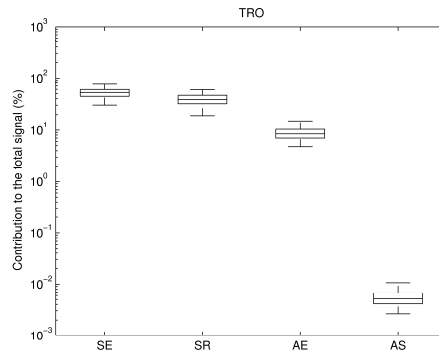


**Figure 1: Contribution to the MIR signal due to surface emission (SE), surface reflection (SR), atmospheric emission (AE) and atmospheric scattering (AS) for TRO atmospheric profile, considering all simulations.**

Levels of noise to be introduced into the MODIS channel were based on the noise equivalent temperature (NEAT) at 300K of channel 20 (0.05 K) that were converted to the respective noise equivalent radiance (NE $\Delta$ L). Randomly generated perturbations were then added to the simulated TOA radiances. Added perturbations are normally distributed around zero mean and with standard deviations equal to the respective MODIS channel NE $\Delta$ L. In order to get statistically significant results, we have generated a set of 1000 random perturbations.

The effects of uncertainties in the humidity and temperature profiles can be analyzed by comparing the radiation at the TOA for a perturbed profile with the radiance for the reference profile. Because the results will depend on the reference (non-perturbed) profile, the experiment adopts the three standard atmospheres stored at MODTRAN-4, namely, TRO, MLS and MLW. A possible way to take into account the errors in the atmospheric profiles might consist in perturbing each atmospheric profile level with values randomly taken from a normal distribution of zero mean and a standard deviation characteristic of the uncertainty. In this case, perturbations on temperature and water vapor are assumed to be independent from each other and values of both quantities at a given level are also taken as independent from those at the other levels, but such procedure is not realistic. An extreme opposite procedure would be considering the perturbations to be perfectly correlated, e.g., by using perturbed profiles that are offset by given amounts (Tjemkes & Schmetz, 1998). In our case, we intend to perform a sensitivity study reflecting more realistic situations. Accordingly, following Peres and DaCamara (2004), the effect of the atmospheric profile source of error was obtained by perturbing the profiles with values based on the background error covariance matrix used in the assimilation schemes of the Global Circulation Model operated at the European Centre for Medium-Range Weather Forecast (ECMWF) (Fillion & Mahfouf, 2000). The covariance coefficients are computed statistically using National Centres for Environment Predictions (NCEP) method based on 24/48-hour forecast differences of the ECMWF model. The background refers to a short-range forecast, which has been started from the analysis at the previous assimilation cycle and is used, in conjunction with a set of observations, to help finding the new analysis state.

Accordingly, three sets of temperature and humidity perturbed profiles based on TRO, MLS and MLW were generated based on the background error covariance matrix of the current operational 4D-Var data assimilation scheme at ECMWF. The imposed perturbations on the atmospheric profiles translate into uncertainties on the atmospheric parameters in equation (3), namely, one-way total atmospheric transmittance, two-way total atmospheric transmittance, upward atmospheric radiance and downward atmospheric radiance.

Radiative transfer computations were performed for the standard profiles, and then errors associated to the inaccuracies in  $T_s$  were introduced RTE. The errors are generated based on accuracy specifications for MODIS LST (1 K) at 1 km resolution under clear-sky conditions (Wan, 1999). The generated errors are normally distributed around zero mean and with standard deviations equal to the respective accuracy specifications for MODIS LST. As in the above mentioned sensitivity studies, we have generated a set of 1000 random perturbations to guarantee a statistically significant result.

For each considered atmospheric and geometry condition (Figures 2 to 4), we have computed the total error in MIR reflectance as obtained using RTE, i.e. equation (3) and the corresponding total error as obtained using KFE, i.e. equation (5).

Results clearly point out that RTE works better than KFE for virtually all atmospheric conditions and geometries. The exceptions correspond to low sun elevations, especially for TRO and MLS atmospheres. It may be noted that SZA has a considerable impact on the accuracy of the estimated reflectance. Low sun elevations induce the largest errors, particularly at high temperatures. This interesting aspect is investigated in Libonati et al. (submitted for publication) where an assessment is performed on the effects of illumination geometry on the retrieval of MIR reflectance using RTE.

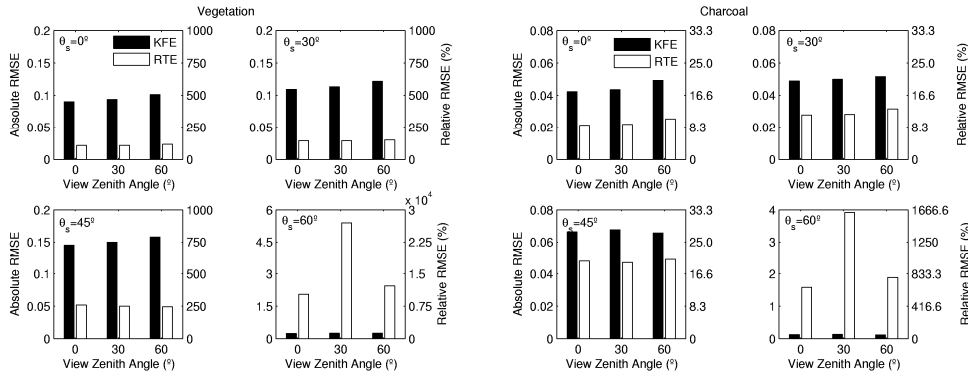


**Figure 2 – Comparison between the total errors of each method analyzed in this study in the case of TRO.**

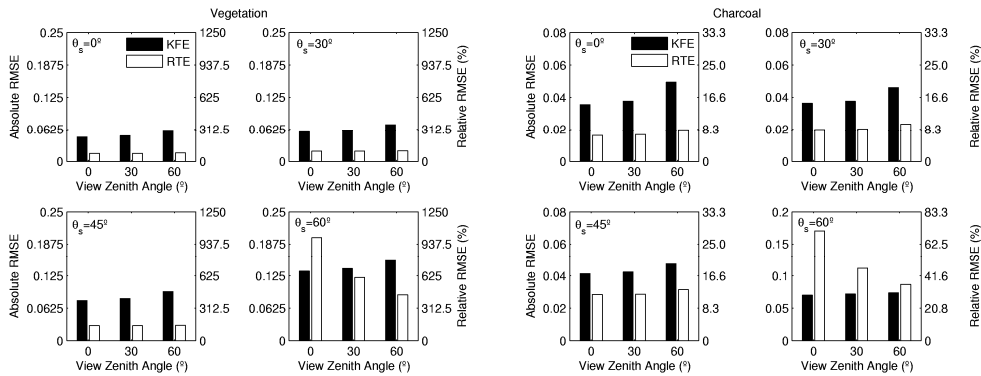


**Figure 3 – Same as Figure 2 but in the case of MLS.**

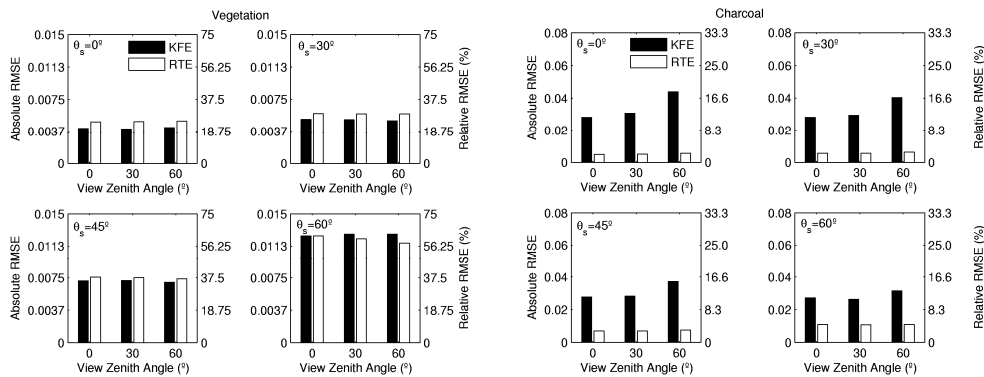


**Figure 4– Same as Figure 2 but in the case of MLW.**

## CONCLUDING REMARKS

The major advantage of the methodology provided by Kaufman and Remer (1994) is to enable for a retrieval of MIR reflectance without the need for auxiliary datasets (e.g. atmospheric profiles) and major computational means (e.g. for radiative transfer computations). However, when using such simplified approaches, one has to take into account several different aspects such as i) the purpose of the application, ii) the season of the year, iii) the location of the study area and iv) the type of target to be identified. In the present case of burned area discrimination in tropical environments, the assumptions of neglecting the atmospheric contributions and of setting the transmittance to unity will have an undesirable impact on the quality of results, in particular when the atmospheric column is contaminated by the presence of heavy smoke layers from biomass burning. Consequently, KFE will be appropriate for cold and dry atmospheres and should be used with care in the case of hot and wet atmospheric conditions. In fact, results shown in Figure 2 clearly show that, in the case of TRO, the prescribed hypotheses by Kaufman and Remer (1994) lead to errors of the same order of magnitude as the one of the reflectance to be estimated, reaching, in some cases, one order of magnitude higher than this value, especially for vegetated surfaces. This feature may therefore severely impair the usage of Kaufman and Remer's algorithm for burnt area discrimination over tropical regions such as Amazonia.

It may be finally stressed that, especially in the case of tropical environments, our results clearly point out that an accurate estimation of MIR reflectance from space data has to rely on the inversion of the general radiative transfer equation, which requires a proper characterization of the atmospheric (e.g., absorption and emission) processes as well as an adequate estimation of land surface temperature. The lack of information about the atmospheric state (humidity and temperature profiles) and about the land surface temperature will prevent any attempt to recover accurate MIR reflectance and to use MIR information for discriminating burned areas.

## **ACKNOWLEDGEMENTS**

The Portuguese Foundation of Science and Technology (FCT) has supported the research performed by the first author (Grant No. SFRH/BD/21650/2005).

## **REFERENCES**

- Barbosa, P.M., Gregoire, J.-M., & Pereira, J.M.C. (1999). An algorithm for extracting burned areas from time series of AVHRR GAC data applied at a continental scale. *Remote Sensing of Environment*, 69, 253–263
- Berk, A., Anderson, G.P., Acharya, P.K., Chetwynd, J.H., Bernstein, L.S., Shettle, E.P., Matthew, M.W., & Alder-Golden, S.M. (2000). MODTRAN4 version 2 user's manual. Air Force Research Laboratory, Space Vehicles Directorate, Air Force Materiel Command, Hanscom AFB, MA 01731-3010
- Boyd, D.S. (1999). The relationship between the biomass of Cameroonian tropical forests and radiation reflected in middle infrared wavelengths (3.0-5.0  $\mu$  m). *Int. J. Remote Sensing*, 20, 1017-1023
- Boyd, D.S., & Duane, W.J. (2001). Exploring spatial and temporal variation in middle infrared reflectance (at 3.75  $\mu$  m) measured from the tropical forests of West Africa. *Int. J. Remote Sensing*, 22, 1861–1878
- Cihlar, J., Latifovica, R., Chena, J., Trishchenko, A., Duc, Y., Fedosejevs, G., & Guindona, B. (2004). Systematic corrections of AVHRR image composites for temporal studies. *Remote Sensing of Environment*, 89, 217–233
- Fillion, L., & Mahfouf, J.F. (2000). Coupling of moist-convective and stratiform precipitation processes for variational data assimilation. *Monthly Weather Review*, 128, 109–124

- Gesell, (1989). An algorithm for snow and ice detection using AVHRR data: An extension to the APOLLO software package. *Int. J. Remote Sensing*, 10, 897–905
- Holben, B.N., & Shimabukuro, Y.E. (1993). Linear mixing model applied to coarse spatial resolution data from multi-spectral satellite sensors. *Int. J. Remote Sensing*, 14, 2231–2240
- Kaufman, Y. J., & Remer, L. (1994). Detection of forests using mid-IR reflectance: An application for aerosol studies. *IEEE Transactions on Geoscience and Remote Sensing*, 32(3), 672-683
- Libonati, R, DaCamara C.C., Pereira, J.M.C., Setzer A.W. & Peres, L.F. (submitted to publication). Problems in retrieving 3.9  $\mu\text{m}$  reflectance in tropical environments. Submitted to *IEEE Geoscience and Remote Sensing Letters*.
- Pereira, J.M.C. (1999). A comparative evaluation of NOAA/AVHRR vegetation indexes for burned surface detection and mapping. *IEEE Transactions on Geoscience and Remote Sensing*, 37(1), 217-226
- Peres, L.F., & DaCamara, C.C. (2004). Land surface temperature and emissivity estimation based on the two-temperature method: sensitivity analysis using simulated MSG/SEVIRI data. *Remote Sensing of Environment*, 91, 377-389
- Roy, D.P., Giglio, L., Kendall, J. D., & Justice, C.O. (1999). Multi-temporal active-fire based burn scar detection algorithm. *Int. J. Remote Sensing*, 20, 1031–1038
- Ruff, I., & Gruber, A. (1983). Multispectral identification of clouds and earth surfaces using AVHRR data. In: *Proceedings of the 5th Conference on Atmospheric Radiation*, Baltimore, MD, October 31–November 4, American Meteorological Society, Boston, MA, pp. 475–478
- Salisbury, J.W., & D'Aria, D.M. (1994). Emissivity of terrestrial materials in the 3-5  $\mu\text{m}$  atmospheric window. *Remote Sensing of Environment*, 47, 345-361
- Tjemkes, S.A., & Schemetz, J. (1998). Radiative transfer simulations for the thermal channels of METEOSAT second generation, EUM TM 01.
- Wan, Z. (1999). MODIS Land-Surface Temperature Algorithm Theoretical Basis Document. Version 3.3, NAS5-31370, NASA/GSFC, Greenbelt MD, USA. Available in: <[http://modis.gsfc.nasa.gov/data/atbd/atbd\\_mod11.pdf](http://modis.gsfc.nasa.gov/data/atbd/atbd_mod11.pdf)> .